



Effect of nanometer SiC coating on thermal conductivity and bending strength of graphite flake/6063Al composites



T. Li^{a,b}, Z.Y. Liu^a, Y.N. Zan^a, X.Y. Liu^c, W.G. Wang^{a,b,*}, D. Wang^{a,**}, B.L. Xiao^a, Z.Y. Ma^a

^a Shi-changxu Innovation Center for Advanced Materials, Institute of Metal Research, Chinese Academy of Sciences, 72 Wenhua Road, Shenyang 110016, China

^b Liaoning Shihua University, No.1 Dandong Road, Fushun 113001, China

^c Shenyang Ligong University, NO.6, Nanping Central Road Hunnan New District, Shenyang 110159, China

ARTICLE INFO

Article history:

Received 22 April 2020

Received in revised form 10 November 2020

Accepted 17 November 2020

Available online 21 November 2020

Keywords:

G_f/Al composite

SiC coating

Sol-gel method

Thermal conductivity

Bending strength

ABSTRACT

SiC coating on graphite flake (G_f) was prepared by SiO₂ sol-gel method combining with in-situ reaction. Then, the SiC coated graphite flakes reinforced 6063Al (SiC@G_f/6063Al) composites were fabricated by vacuum hot pressing method. The results demonstrated that the SiC coating with a thickness of about 15 nm on the G_f could effectively improve the wettability, reduce the interface thermal resistance, and enhance the bonding between G_f and Al matrix. As a result, the bending strength as well as the thermal conductivity of the SiC@G_f/6063Al composites was much higher than those of the G_f/6063Al composites. Especially, the 50 vol% SiC@G_f/6063Al had the highest bending strength of 52.5 MPa, and the thermal conductivity of the 70 vol% SiC@G_f/6063Al reached the highest value of 731.4 W m⁻¹ K⁻¹.

© 2020 Elsevier B.V. All rights reserved.

1. Introduction

Thermal management challenge become serious concern in microelectronic technology because of the constantly growing power density and continuous miniaturization of electronic devices [1], which could raise device temperature severely and were not beneficial to the normal operation of electronic components. To meet the demand for electronic packaging materials with high performance, it is necessary to develop advanced thermal management materials which have high thermal conductivity (TC), low coefficient of thermal expansion (CTE) as well as good mechanical properties [2,3].

Excellent TC and thermal diffusivity are necessary for effectively dissipating heat generated by microelectronic devices. For some traditional materials such as pure aluminium and copper, although they have good TC, the CTE of them is as high as $23.6 \times 10^{-6} \text{ K}^{-1}$ and $17.8 \times 10^{-6} \text{ K}^{-1}$, respectively. Then, a large mismatch of CTE between thermal management materials and semiconductor substrate (such as Si widely used in optoelectronic devices, $4.1 \times 10^{-6} \text{ K}^{-1}$) would be formed [4]. Further, the

mismatch would lead to large internal stress in components during the thermal cycling, even if format some defects such as internal micro-pores, cracks or other defects. In order to reduce the CTE of the materials, e.g. Al-SiC [5], Cu-Mo [6] and other materials were used wildly in the thermal management field as the second generation of thermal management materials. However, the reduction in the thermal expansion coefficient came at the expense of TC. In a word, these traditional materials could not meet the needs of rapidly developing highly integrated microelectronics devices because of either high CTE or relatively low TC, so it is urgent to develop a new generation of thermal management materials.

Metal matrix composites (MMCs), properties of which could be tailored by adding appropriate reinforcements, have obvious advantages as thermal management materials. Several carbon-based materials such as diamonds, carbon nano-tubes (CNT), carbon fibers (CF) or graphite flakes (G_f) are promising reinforcements for thermal management applications due to their outstanding TC and low CTE [7–10].

Diamonds have the highest TC among the natural materials, which can reach $2,500 \text{ W m}^{-1} \text{ K}^{-1}$. In the past few decades, researches have shown that diamond/metal composites exhibited excellent TC, which could be $350\text{--}700 \text{ W m}^{-1} \text{ K}^{-1}$ [11,12] and the CTE is $1.3 \times 10^{-6} \text{ K}^{-1}$ [7]. However, difficult machining limited its application. The TC of CNT [13] and CF [14] could reach $3,000 \text{ W m}^{-1} \text{ K}^{-1}$ and $1,000 \text{ W m}^{-1} \text{ K}^{-1}$, respectively. Unfortunately,

* Corresponding author at: Shenyang National Laboratory for Materials Science, Institute of Metal Research, Chinese Academy of Sciences, Shenyang 110016, China

** Corresponding author.

E-mail addresses: wgwang@imr.ac.cn (W.G. Wang), dongwang@imr.ac.cn (D. Wang).

both of them belong to one-dimension material, the high TC could only exist in axial direction [15–17], which constrains the application of the CNT or CF composites in the thermal management field.

Natural G_r is a carbon material with a typical two-dimensional structure and has good machinability. Particularly, the TC parallel to $(001)_{\text{Graphite}}$ can reach $1,000 \text{ W m}^{-1} \text{ K}^{-1}$ [18], which makes it an ideal reinforcement for thermal management composites. Nevertheless, the TC perpendicular to $(001)_{\text{Graphite}}$ is only $38 \text{ W m}^{-1} \text{ K}^{-1}$ [19]. So optimizing the orientation of G_r is necessary, which can enormously improve the TC of the composites [20–24]. Furthermore, the poor wettability and bonding strength, high thermal resistance between G_r and Al matrix result in weak mechanical properties [25] and degradation of thermal transfer efficiency [19]. On the other side, it is very difficult to avoid the interfacial reaction between Al matrix and carbon reinforcements during fabrication at relatively high temperatures, and the interface reaction product of Al_4C_3 is also harmful to the TC and mechanical properties [26]. In addition, Al_4C_3 is easy to hydrolyze in a wet atmosphere, which will seriously threaten the safety of the composite application. Therefore, the main technical problem of G_r/Al could be summarized as bad wettability, weak interface bonding, serious interfacial reaction and high interface thermal resistance. Plenty of methods have been developed for solving the above problems. Coating of TiC, WC or SiC on G_r is usually introduced to modify the G_r -Metal interfaces.

Wang et al. [27] coated carbide (SiC/TiC) on the surface of the G_r by the salt bath method. It was found that TC and bending strength of composites were improved. Moreover, the coating of G_r/Al composites hinders interfacial reaction. Xue [28] used the same technique to modify the G_r surfaces with SiC coating. Through this method, the TC and bending strength of G_r/Al materials are effectively improved. Nevertheless, this technique needs Si to be placed in CaCl_2 , and then the prepared mixture headed to $1,100 \text{ }^\circ\text{C}$ for 1 h in an argon atmosphere. After heat-treatment, the coated G_r were separated from the mixture by screening and cleaned in the distilled water for eliminating the CaCl_2 , following drying at $100 \text{ }^\circ\text{C}$. Finally, the SiC coating with a thickness of 250 nm was obtained. Up to now, there are still few reports on the research using the molten salt method. Although, SiC coating showed a good effect of interfacial modification in G_r/Al composites, a novel method to prepare carbide coating is still desirable, which has the advantages of simple process, environmentally friendly, precise and controllable coating, etc.

In this article, aiming at the problem of poor wettability, weak interfacial bonding and the interfacial reaction between G_r and Al matrix, nano SiC coating on G_r was prepared by sol-gel method combining with in-situ reduction method. And then G_r/Al composites were prepared by vacuum hot pressing. The microstructure of G_r coating, the effect of nano-scale SiC coating on TC and bending strength of the composites were investigated.

2. Experimental procedure

2.1. Materials and methods

The as-received 6063Al powders (Al-Mg-Si) with the particle size in the range of 5–13 μm were purchased from Angang Group Aluminium Powder Co., Ltd. The G_r powders with an average diameter of 500 μm and thickness of 30 μm were provided by Shandong Yuyang new energy Co., Ltd. The chemical reagents, tetraethyl orthosilicate (TEOS), anhydrous ethanol ($\text{C}_2\text{H}_5\text{OH}$, 99.8 wt%), concentrated nitric acid (HNO_3 , 68 wt%), deionized water were supplied by Sinopharm Group Co., Ltd.

The SiC coating on the G_r was fabricated by sol-gel method. The G_r with SiC coating were prepared as follows: Firstly, TEOS, $\text{C}_2\text{H}_5\text{OH}$ and H_2O were mixed with the molar ratio of 1:5:16, and then HNO_3 was added to the mixed solution to adjust the pH value of the solution to 2.8. Under magnetic stirring, the solution was heated in a water bath

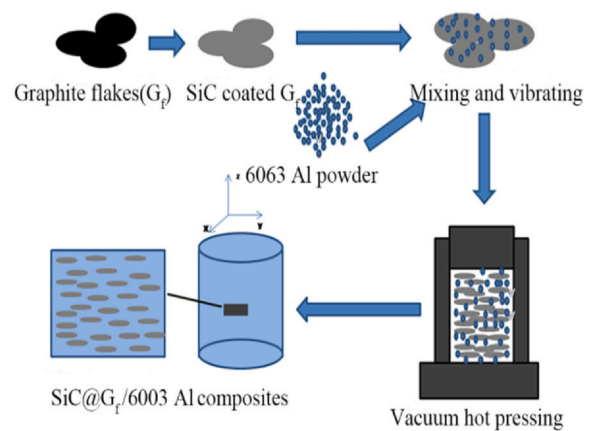


Fig. 1. The process of SiC@ G_r/Al composite preparation.

for 8 h to obtain a uniform sol. Secondly, the G_r were stirred in the sol for 10 min and dried at room temperature for 3 days. Finally, the prepared G_r were put into a graphite mould with a high temperature of $1,800 \text{ }^\circ\text{C}$ for 180 min in a vacuum atmosphere to form the SiC coated G_r (SiC@ G_r).

The fabricating procedure of $G_r/6063\text{Al}$ composites was shown in Fig. 1. The SiC@ $G_r/6063\text{Al}$ composites were fabricated by vacuum hot pressing method. Firstly, the SiC@ G_r and 6063Al powders were mixed at room temperature using a rotation mixer at a speed of 50 rpm for 10 min. Then, the mixtures were filled into a steel mould, vibrated on a shaking platform for 2 h with the frequency of 100 Hz to ensure the orientation of G_r and followed by cold compacting. Finally, the composites of cold consolidated were heated to $620 \text{ }^\circ\text{C}$ and held for 120 min in a vacuum of 10^{-2} Pa and then pressed at 100 MPa, producing the composite sample with 50 mm in diameter and 50 mm in height. The composite reinforced by the SiC-coated G_r is denoted as SiC@ G_r/Al . Meanwhile, the G_r without SiC coating were also used to produce a composite in the same powder metallurgy route, denoted as G_r/Al .

2.2. Characterization

The microstructure and interface of the composites were observed by scanning electron microscopy (SEM, ZEISS SUPRA 55) and metallurgical microscope (OM, Axiovert 200 MAT). X-ray diffraction (XRD, D/max 2500PC) was applied to identify the phase of SiC@ $G_r/6063\text{Al}$ composites. The thickness of SiC coating G_r was observed by transmission electron microscopy (TEM, FEI TECNAI F20). X-ray photoelectron spectroscopy (XPS, ESCALAB250) was carried out to determine the composition of the coating. The laser-flash method (NETZSCH LFA447, Germany) was used to measure TC. The TC was calculated according to the formula $\lambda = \alpha C_p \rho$ (where: λ -the TC of the composite, $\text{W m}^{-1} \text{ K}^{-1}$; α -thermal diffusion coefficient, $\text{m}^2 \text{ s}$; C_p -specific heat, $\text{J kg}^{-1} \text{ K}^{-1}$; ρ -density of composite materials, g m^{-3}). The TC measured was perpendicular to the hot pressing direction. The density was measured using the Archimedes principle by DX-100E. The bending strength parallel and perpendicular to the hot pressing direction was measured ($3 \times 4 \times 30 \text{ mm}$), respectively, using AG-I 500KN.

3. Results and discussion

3.1. Microstructure and characterization of SiC@ G_r

Fig. 2(a) shows the SEM images of the as-received G_r with an average diameter of 500 μm . Fig. 2(b) reveals the surface morphology of the SiC@ G_r powders. It could be seen that SiC coating on

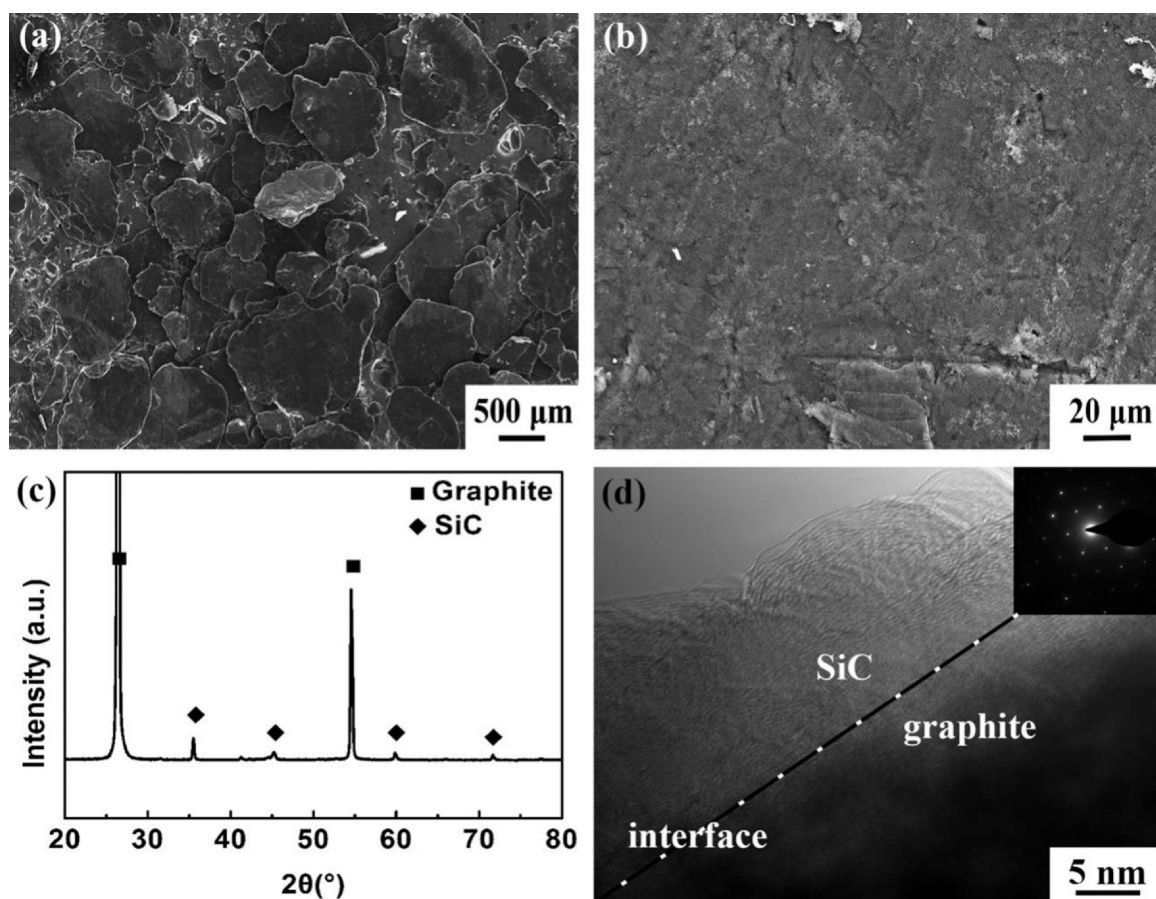


Fig. 2. (a) Morphology of original graphite flake, (b) magnified surface morphology of SiC coated graphite flake, (c) XRD of SiC coated graphite flake and (d) SiC coating on graphite surface.

the G_f surface exhibited a uniform distribution without rupture or fold, indicating the high quality of the SiC coating. XRD pattern of SiC@ G_f is shown in Fig. 2(c). Apart from graphite, the peaks of SiC occurring at about $2\theta = 35.58^\circ$ and 60° could be observed. It implied the existence of SiC coating. No peak of other phases could be found in the XRD pattern, which indicated no impurity. Fig. 2(d) shows the SiC coating structure on G_f under TEM. The thickness of SiC coating is about 15 nm and no pore could be observed.

In order to further investigate the ingredient of the coating, SiC@ G_f was detected by XPS, as shown in Fig. 3(a). The XPS survey spectra of SiC@ G_f , which exhibits five peaks assigned to Si 2p, Si 2s, C 1s, O 1s. The deconvolution of the Si 2p peak is shown in Fig. 3(b). Only one peak at 100.7 eV corresponding to Si\C [17] was detected, while the Si\Si (99.6 eV) or Si\O (103.2 eV) peak was not detected, which demonstrated that the surface of coated G_f was free of Si and SiO₂. Fig. 3(c) shows the deconvolution of C 1s peaks and it also exhibited the content percentage of carbon-containing compounds. The peaks at 283.4 and 284.6 eV correspond to C\Si and C\C, respectively. The existence of C\Si and Si\C peaks in the deconvolution of the C 1s and Si 2p peaks demonstrates that SiC was formed at high temperatures. There is no Si\O peak, which means that C and SiO₂ reacted adequately. Fig. 3(d) shows the coating structure and reaction process between G_f and SiO₂ coating, and the interfacial reaction between the SiO₂ coating and G_f obeyed the Eq. (1). Because the interface reaction could be considered as a gradual process, the Eq. (1) could be decomposed into two steps. At first, the SiO₂ contacting with the G_f directly reacted with the carbon element to form SiC, resulting in the isolation of SiO₂ and G_f . Secondly, the carbon element diffused to the SiO₂ side at 1,800 °C, and then some reduced Si element (obeyed by Eq. (2)) diffused to the G_f side and acted with

carbon element to form SiC (Eq. (3)). Therefore, the interface between G_f and SiC were well bonded.

3.2. Microstructure and the interface of SiC@ G_f /6063Al composites

Fig. 4 shows the microstructure of the SiC@ G_f /6063Al composites with G_f volume fraction of 50%, 60%, 70% and 80%. The black areas represent the G_f while the white districts are the Al matrix. No micro-pore or micro-crack was observed, indicating a high-quality G_f /Al interface and dense composite. The structure of composites exhibited obvious lamellar morphology. The G_f were uniformly distributed and exhibited a preferred orientation arrangement. With the increase of G_f volume fraction, the degree of G_f orientation became better. However, some contact between the G_f could be observed with the increasing volume fraction of G_f and some G_f were even bent (Fig. 4(d)), especially as the G_f volume fraction reached 80%. It is a universal phenomenon in a composite with high graphite volume fraction [27,29]. The path of thermal conduction will be blocked due to the bending of the graphite, which is adverse to the heat transfer on G_f .

XRD pattern shown in Fig. 5 further confirmed the composition of the composites. It can be observed from XRD patterns of SiC@ G_f /6063Al composite that the graphite diffraction peaks were detected at about $2\theta = 26.5^\circ$ and the diffraction peaks of Al and SiC could be also detected, without Al₄C₃ phase. Generally, Al₄C₃ phase was frequently found in the C-Al composites [29], which would absorb moisture in the air easily, resulting in reduced mechanical properties. However, the peaks of Al₄C₃ phase were not detected in SiC@ G_f /6063Al by XRD. It means that the coating of SiC on G_f could prevent

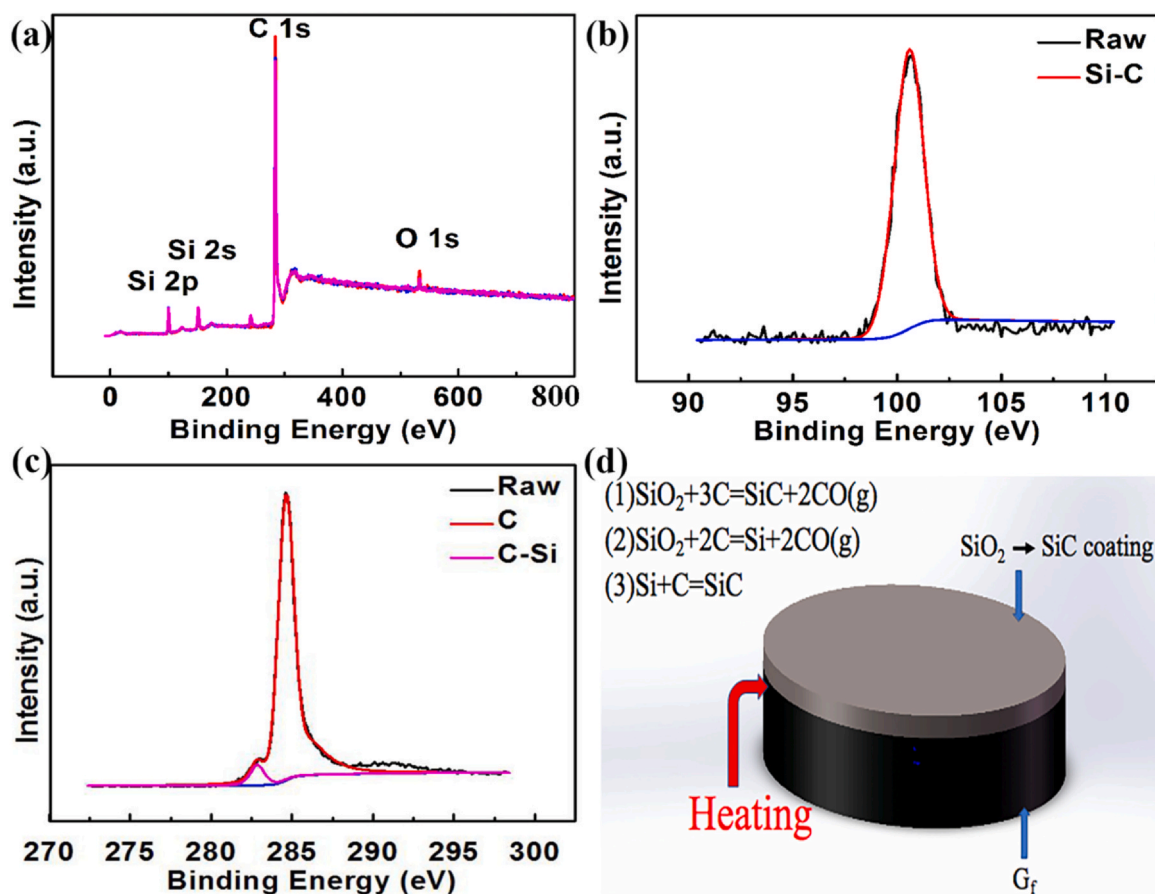


Fig. 3. XPS spectra of (a) as prepared graphite, (b) the corresponding Si 2p, (c) the corresponding C 1s and (d) the coating structure and reaction process between G_f and SiO_2 coating.

direct contact between Al and G_f , constraining the formation of interfacial product Al_4C_3 .

3.3. Thermal conductivity and bending strength

The TC of $SiC@G_f/6063Al$ composite was determined by density, specific heat and thermal diffusivity. The TC of the composites can be calculated according to the following formula $\lambda = \alpha \cdot C_p \cdot \rho$ described in Section 2.2.

The TC of composites with different volume fractions of G_f are shown in Table 1. It should be mentioned that G_f is an anisotropic material, so the TC was measured along $(001)_{Graphite}$ plane with the highest TC. It is widely known that the G_f owns higher thermal conductive compared with Al, thus the thermal conductive of the composite was increased by the addition of the G_f . The diameter of G_f is as large as $500 \mu m$, which is a benefit to obtain a smaller interface thermal resistance, by reducing the number of interfaces. As the G_f content increasing from 50 to 70 vol%, TC of composites increased from $420 W m^{-1} K^{-1}$ to $731.4 W m^{-1} K^{-1}$. Comparing with the $G_f/6063Al$ composites without G_f coating, the TC of the obtained composites was increased by about 11% in composites with a different volume fraction of G_f . When the G_f volume fraction reached 70%, the maximum of TC was obtained. However, when the G_f fraction got to 80%, the TC of the composites decreased to $563.0 W m^{-1} K^{-1}$. It ought to be attributed mainly to two reasons. On the one hand, an excess volume fraction of G_f led to insufficient aluminium, which destroyed the interfacial bonding of adjacent G_f . G_f could contact directly with each other, resulting in increased thermal resistance at the interface. On the other hand, at high

volume fraction, the lamellar graphite flakes were bent, thus blocking the thermal conducting path and resulting in a sharp decrease in TC. It was believed that the TC of the composites could be enhanced by solving the graphite bending problem and arranging the flakes in a good orientation.

The bending strength reduced as the volume fraction of the G_f increased, as shown in Table 1. The strength of G_f is much lower than that of Al and therefore decreased the bending strength of the composites. There is no effective method to enhance the bending strength and TC of the composite simultaneously for a given volume fraction of the graphite up to now. However, the composites with SiC coating showed a bending strength of about 20% higher than those without SiC coating. It demonstrates that SiC coated on the surface of the G_f significantly improved the interfacial bonding between G_f and Al.

It can be observed from Fig. 6(a) for the interface of the $SiC@G_f/Al$ composite. The results show a clean and strong interfacial bonding between G_f and Al. The junction between G_f and Al is the interfacial layer. To further study the interfacial structure of $SiC@G_f/Al$, the element distribution on the interface is detected and shown in Fig. 6(b). The result shows that Al, C and Si elements all existed in the interface region, and diffusion of Si and Al was also observed from Fig. 6(b). The interfacial SiC can improve the wettability of the two phases, enhance the interfacial bonding, facilitate the energy exchange between metal and carbon, and reduce the high interfacial thermal resistance at the carbon-metal interface due to the mismatch of vibration modes.

Fig. 7 shows the fracture morphology of the 70 vol% $SiC@G_f/6063Al$ and $G_f/6063Al$ composites. The composites exhibited pronounced layer fracture characteristics. Local magnification images of

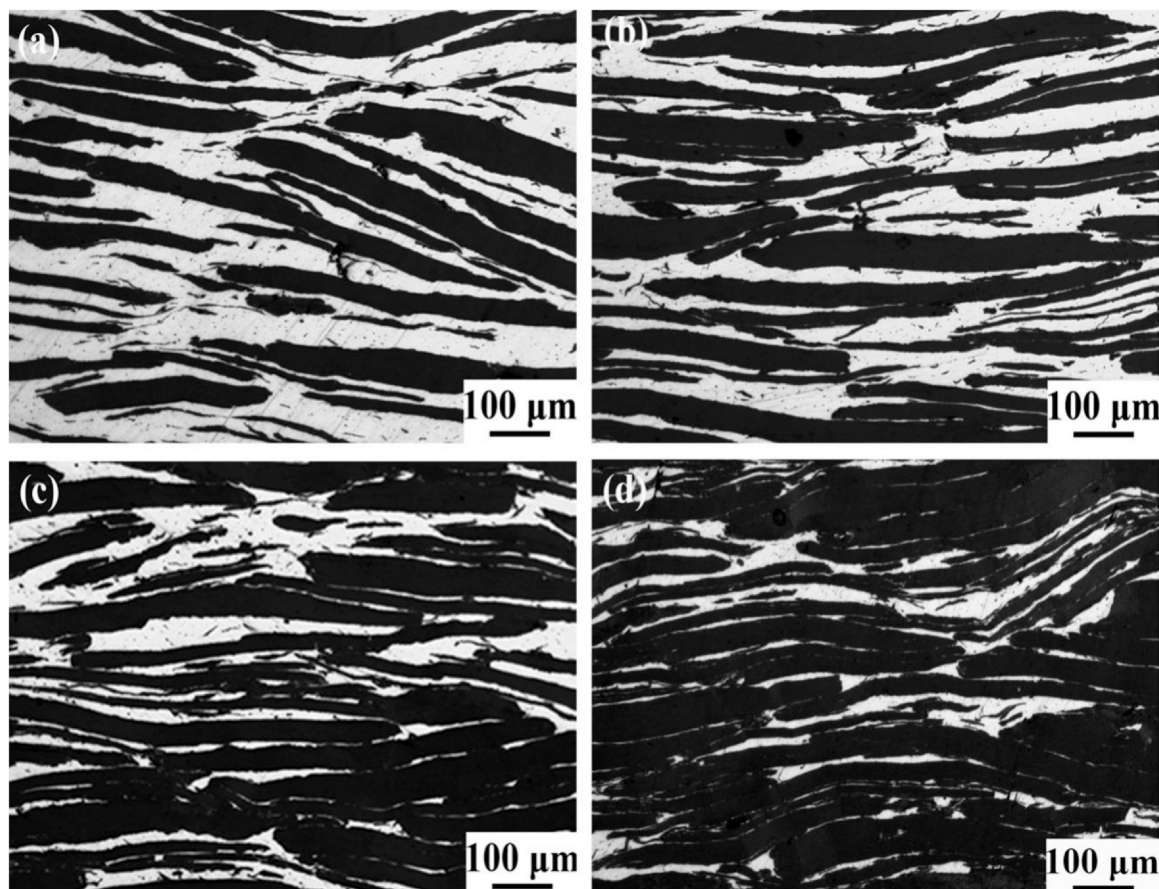


Fig. 4. Microstructure of graphite-SiC/Al composite with graphite volume fraction of (a) 50%, (b) 60%, (c) 70%, and (d) 80%.

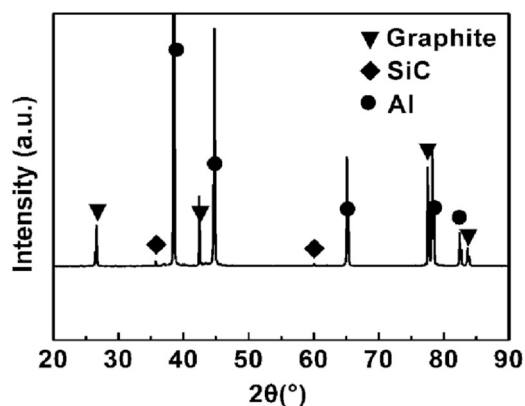


Fig. 5. XRD patterns of SiC@G_f/6063Al composite.

the fracture surface are shown in Fig. 7(b) and (d). In 70 vol% SiC@G_f/6063Al, many fractured G_f could be observed. As a contrast, for the 70 vol% G_f/6063Al composite, most of the G_f on the fracture surface were of peeling states. It also proved that the SiC coating could effectively improve the interfacial strength between G_f and Al matrix. In a word, the existence of SiC coating on G_f played a significant role in improving the TC and the bending strength.

4. Conclusion

G_f with nano-scale SiC coating were obtained by sol-gel combined with thermal reduction reaction processing. And then SiC@G_f/6063Al composites with aligned G_f and well interface bonding were achieved by powder metallurgy. No detrimental Al₄C₃ formed in the SiC@G_f/6063Al composites.

By forming SiC coating on G_f, the TC and the bending strength of the composites was respectively 10% and 20% higher than that of the composites without SiC coating. With increasing the graphite content from 50 to 80 vol%, the TC of composites firstly increased and

Table 1
Thermal conductivities and bending strengths of graphite/Al composites.

Volume fraction of G _f	TC (W m ⁻¹ K ⁻¹)		Bending strength (MPa)			
	∥ (001) _{Graphite}		∥ (001) _{Graphite}		⊥ (001) _{Graphite}	
	NO Coating	Coating	NO Coating	Coating	NO Coating	Coating
50%	501.0	540.0	48.8	52.5	6.2	6.6
60%	551.7	627.4	40.3	45.1	4.1	4.4
70%	640.0	731.4	36.2	40.1	2.2	4.4
80%	515.7	563.0	21.4	26.6	2.1	2.6

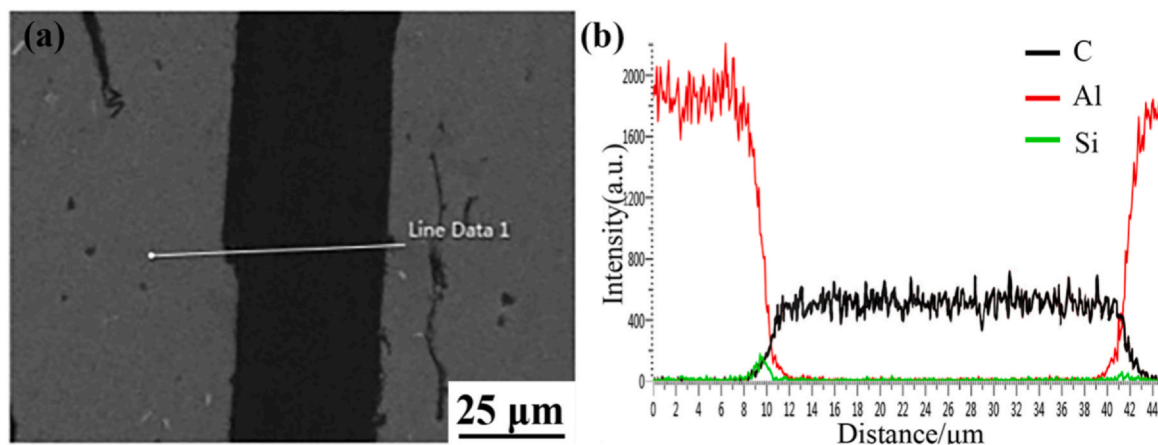


Fig. 6. Interfacial observation of SiC@Gf/Al composite: (a) SEM observation, (b) element distribution of line scanned on interface.

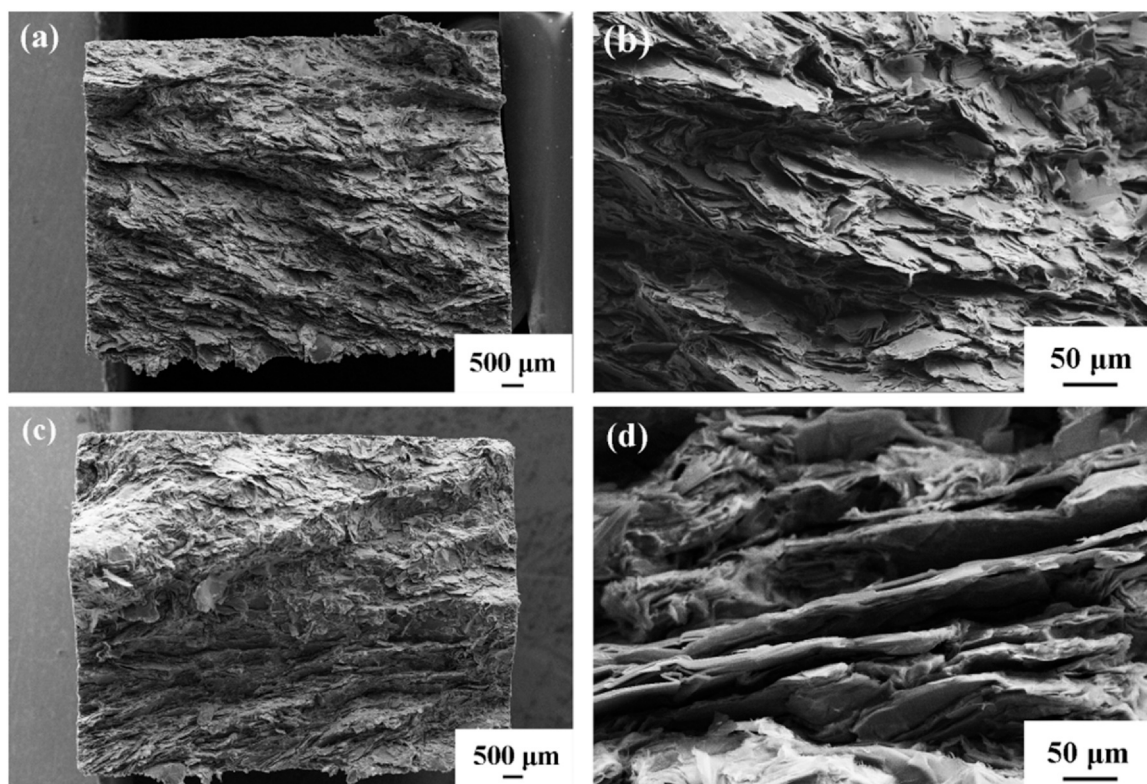


Fig. 7. Fracture morphology of (a), (b) 70 vol% SiC@Gf/6063Al composites and (c), (d) 70 vol% Gf/Al composites.

then decreased. When the graphite volume fraction reached 70%, the TC got to the maximum value ($731.4 \text{ W m}^{-1} \text{ K}^{-1}$). Though the in-situ SiC coating was very thin, it could play a significant role in controlling interfacial reaction and modifying the interfacial wettability and compatibility, resulting in improved thermal and mechanical properties of SiC@Gf/6063Al.

CRediT authorship contribution statement

Tong Li: Methodology, Investigation, Visualization, Writing - original draft. **Zhenyu Liu:** Investigation, Writing - original draft. **Yuning Zan:** Visualization, Data curation. **Xiaoyun Liu:** Investigation. **Wenguang Wang:** Project administration, Funding acquisition. **Dong Wang:** Resources, Supervision. **Bolv Xiao:**

Conceptualization. **Zongyi Ma:** Writing - review & editing, Funding acquisition.

Declaration of Competing Interest

The authors declare that they have no known competing financial interests or personal relationships that could have appeared to influence the work reported in this paper.

Acknowledgments

The authors gratefully acknowledge the support of (a) Key Research Program of Frontier Sciences, Chinese Academy of Sciences (No. QYZDJ-SSW-JSC015), (b) National Key R & D

Program of China under grant of No. 2017YFB0703104, and (c) the National Natural Science Foundation of China under grant No. 51931009.

References

- [1] A.M. Abyzov, S.V. Kidalov, F.M. Shakhov, High thermal conductivity composite of diamond particles with tungsten coating in a copper matrix for heat sink application, *Appl. Therm. Eng.* 48 (2012) 72–80.
- [2] Q. Liu, X.B. He, S.B. Ren, Thermophysical properties and microstructure of graphite flake/copper composites processed by electroless copper coating, *J. Alloys Compd.* 587 (2014) 255–259.
- [3] C. Zhou, W. Huang, Z. Chen, In-plane thermal enhancement behaviors of Al matrix composites with oriented graphite flake alignment, *Compos. Part B* 70 (2015) 256–262.
- [4] Q. Huang, M.Y. Gu, Status and prospects of metal matrix composites for electronic packaging, *Electron. Packag.* 3 (2003) 22–25.
- [5] Z.Z. Chen, Z.Q. Tan, G. Ji, Effect of interface evolution on thermal conductivity of vacuum hot pressed SiC/Al composites, *Adv. Eng. Mater.* 17 (2015) 1077–1085.
- [6] J. Stolk, A. Manthiram, Chemical synthesis and characterization of low thermal expansion-high conductivity Cu-Mo and Ag-Mo composites, *Metall. Mater. Trans. A* 31 (2000) 2396–2398.
- [7] R. Prieto, J.M. Molina, J. Narciso, Fabrication and properties of graphite flakes/metal composites for thermal management applications, *Scr. Mater.* 59 (2008) 11–14.
- [8] C. Xue, H. Bai, P. Tao, Analysis on thermal conductivity of Graphite/Al composite by experimental and modeling study, *J. Mater. Eng. Perform.* 26 (2017) 327–334.
- [9] W. Feng, M.M. Qin, Y.Y. Feng, Toward highly thermally conductive all-carbon composites: structure control, *Carbon* 109 (2016) 575–597.
- [10] G. Subhra, S. Niladri, R. Dibyanjan, Design of carbon nanofiber embedded conducting epoxy resin, *Mater. Chem. Phys.* 186 (2017) 29–35.
- [11] H. Bai, N.G. Ma, J. Lang, Thermal conductivity of Cu/diamond composites prepared by a new pretreatment of diamond powder, *Compos. Part B* 52 (2013) 182–186.
- [12] I.E. Monje, E. Louis, J.M. Molina, Optimizing thermal conductivity in gas-pressure infiltrated aluminum/diamond composites by precise processing control, *Compos. Part A* 48 (2013) 9–14.
- [13] S. Berber, Y.K. Kwon, D. Tomanek, Unusually high thermal conductivity of carbon nanotubes, *Phys. Rev. Lett.* 84 (2000) 4613–4616.
- [14] G. Francisco Emmerich, Young's modulus, thermal conductivity, electrical resistivity and coefficient of thermal expansion of mesophase pitch-based carbon fibers, *Carbon* 79 (2014) 274–293.
- [15] C. Kim, B. Lim, B. Kim, U. Shim, S. Oh, B. Sung, J. Choi, J. Ki, S. Baik, Strengthening of copper matrix composites by nickel-coated single-walled carbon nanotube reinforcements, *Synth. Met.* 159 (2009) 424–429.
- [16] Q. Huang, L. Gao, Y.Q. Liu, Sintering and thermal properties of multiwalled carbon nanotube–BaTiO₃ composites, *J. Mater. Chem.* 15 (2005) 1995–2001.
- [17] J.C. Lloyd, E. Neubauer, J. Barcena, W.J. Clegg, Effect of titanium on copper–titanium/carbon nanofibre composite materials, *Compos. Sci. Technol.* 70 (2010) 2284–2289.
- [18] C. Zhou, G. Ji, Z. Chen, M. Wang, A. Addad, D. Schryvers, H. Wang, Fabrication, interface characterization and modeling of oriented graphite flakes/Si/Al composites for thermal management applications, *Mater. Des.* 63 (2014) 719–728.
- [19] R. Prieto, J.M. Molina, J. Narciso, E. Louis, Thermal conductivity of graphite flakes–SiC particles/metal composites, *Compos. Part A* 42 (2011) 1970–1977.
- [20] G. Yuan, X. Li, Z. Dong, A. Westwood, Z. Cui, Y. Cong, H. Du, F. Kang, Graphite blocks with preferred orientation and high thermal conductivity, *Carbon* 50 (2012) 175–182.
- [21] Z. Liu, Q. Guo, J. Shi, G. Zhai, L. Liu, Graphite blocks with high thermal conductivity derived from natural graphite flake, *Carbon* 46 (2008) 414–421.
- [22] S. Zhou, S. Chiang, J. Xu, H. Du, B. Li, C. Xu, F. Kang, Modeling the inplane thermal conductivity of a graphite/polymer composite sheet with a very high content of natural flake graphite, *Carbon* 50 (2012) 5052–5061.
- [23] P.G. Klemens, D.F. Pedraza, Thermal conductivity of graphite in the basal plane, *Carbon* 4 (1994) 735–741.
- [24] M. Murakami, N. Nishiki, K. Nakamura, J. Ehara, H. Okada, T. Kouzaki, K. Watanabe, T. Hoshi, S. Yoshimura, High-quality and highly oriented graphite block from polycondensation polymer-films, *Carbon* 30 (1992) 255–262.
- [25] W. Li, Y. Liu, G. Wu, Preparation of graphite flakes/Al with preferred orientation and high thermal conductivity by squeeze casting, *Carbon* 95 (2015) 545–551.
- [26] T. Etter, P. Schulz, M. Weber, J. Metz, M. Wimpler, J.F. Löffler, P.J. Uggowitzer, Aluminium carbide formation in interpenetrating graphite/aluminium composites, *Mater. Sci. Eng. A* 448 (2007) 1–6.
- [27] C. Wang, H. Bai, C. Xue, X. Tong, Y. Zhu, N. Jiang, On the influence of carbide coating on the thermal conductivity and flexural strength of X (X = SiC, TiC) coated graphite/Al composites, *RSC Adv.* 6 (2016) 107483–107490.
- [28] C. Xue, H. Bai, P.F. Tao, J.W. Wang, N. Jiang, S.L. Wang, Thermal conductivity and mechanical properties of flake graphite/Al composite with a SiC nano-layer on graphite surface, *Mater. Des.* 108 (2016) 250–258.
- [29] J.K. Chen, I.S. Huang, Thermal properties of aluminum–graphite composites by powder metallurgy, *Compos. Part B* 44 (2013) 698–703.